



# Hurricane Harvey Storm Sedimentation in the San Bernard National Wildlife Refuge, Texas: Fluvial Versus Storm Surge Deposition

Qiang Yao<sup>1</sup>  · Kam-Biu Liu<sup>1</sup> · Harry Williams<sup>2</sup> · Sanjeev Joshi<sup>1</sup> · Thomas A. Bianchette<sup>3</sup> · Junghyung Ryu<sup>1</sup> · Marianne Dietz<sup>1</sup>

Received: 18 March 2019 / Revised: 7 August 2019 / Accepted: 11 September 2019  
© Coastal and Estuarine Research Federation 2019

## Abstract

Few studies have documented the characteristics of fluvial flooding-induced storm deposits associated with a modern hurricane. Hurricane Harvey (2017) caused extensive flooding in coastal Texas due to a combination of storm surge and heavy precipitation. This study investigates the depositional process associated with Hurricane Harvey by means of loss-on-ignition (LOI) and X-ray fluorescence (XRF) analyses of 9 short cores and 17 surface samples collected from the San Bernard National Wildlife Refuge (SBNWR), Texas. Hurricane Harvey caused the largest flood within SBNWR over the last 28 years, and freshwater flooding from the San Bernard River was the predominant cause of this inundation. A distinct washover sand layer is lacking at all coring sites, but the intrusion of seawater can still be detected by a peak in the chlorine/bromine (Cl/Br) ratio of most sediment cores. Our study shows that Cl/Br ratios are higher in coastal environments than in terrestrial environments, thereby confirming that this elemental ratio can be used as a salinity indicator and, as a corollary, evidence of marine intrusion into lower-salinity environments. The ensuing phase of freshwater flooding and fluvial sedimentation is represented by a distinct flood deposit in only three cores, but is absent or indistinct in most cores. The elusiveness of the Harvey fluvial flood deposit can be explained by the relatively low discharge and suspended sediment load of the San Bernard River, the uneven distribution of this event deposit, and its indistinctiveness with the underlying deposits laid down by previous flood events.

**Keywords** Hurricane Harvey · Overbank flooding · Flood deposit · Storm surge · Storm sedimentation · Cl/Br ratio

## Introduction

Hurricane Harvey, a category 4 hurricane that first made landfall on the Texas coast on August 25, 2017, is the second costliest hurricane event on record (Blake and Zelinsky 2017). It is the first major hurricane that made landfall in the continental U.S. since Hurricane Wilma in 2005 and the first

intense hurricane of the extremely active 2017 Atlantic hurricane season. Hurricane Harvey not only caused a high storm surge that impacted hundreds of kilometers of coastal zones but also brought catastrophic rainfalls that flooded hundreds of thousands of structures, especially in the Houston metropolitan area (Blake and Zelinsky 2017). Empirical data of the coastal flood event and its associated storm deposits will offer insights to the depositional processes of major hurricane events (Liu 2004). Such information is vital for shoreline protection, coastal wetland restoration, and societal response to hurricane impacts.

During the past two decades, the storm deposition of modern hurricanes has been documented throughout the Gulf of Mexico and Central American coasts. Most of these studies are concerned with storm deposition associated with storm surge or overwash processes (e.g., Williams and Flanagan 2009, Williams 2010, Williams 2012; Lane et al. 2011; Liu et al. 2011, 2014; McCloskey and Liu 2012, 2013; Yao et al. 2015, 2018). However, few studies have documented the stratigraphical and geochemical characteristics of storm deposits caused by fluvial flooding, and even fewer records are

---

Communicated by Mead Allison

 Qiang Yao  
qyao4@lsu.edu

<sup>1</sup> Department of Oceanography and Coastal Sciences, Louisiana State University, Baton Rouge, LA 70803, USA

<sup>2</sup> Department of Geography and the Environment, University of North Texas, Denton, TX 76203, USA

<sup>3</sup> Department of Natural Sciences, College of Arts, Sciences, and Letters, University of Michigan—Dearborn, Dearborn, MI 48128, USA

available on the sedimentary mechanism of rainfall-triggered flooding associated with a modern hurricane (Khan et al. 2013). Hurricane Harvey, a unique hurricane event that combines heavy fluvial flooding and storm surge in Texas, provides an excellent opportunity to fill this data gap. In this study, we present sedimentological and geochemical data from a series of sediment cores and surface samples collected from the San Bernard National Wildlife Refuge (SBNWR) on the east-central coast of Texas, to document the storm deposition attributed to the storm surge and fluvial flooding processes associated with Hurricane Harvey. The sedimentary evidence was interpreted in light of Harvey's hydrological impacts reconstructed by compiling a 28-year time-series of daily discharge data of the San Bernard River during 1990–2017, coupled with the hourly discharge data associated with this storm-triggered flooding event.

### Effects of Recent Hurricanes

During the last two decades, the San Bernard National Wildlife Refuge (SBNWR) has been repeatedly affected by hurricanes and their associated flood and storm surge impacts (NOAA 2018a). In 2003, Hurricane Claudette (category 1) made landfall to the west of the SBNWR with an estimated maximum wind speed of 148 km/h. It caused up to 3-m-high

storm surges along coastlines from central Texas to southwestern Louisiana. In 2007, Hurricane Humberto (category 1) made landfall to the east side of the SBNWR with a sustained wind speed over 150 km/h. It caused up to 2-m-high storm surge as well as very heavy rainfall (maximum total 360 mm) in coastal zones from Galveston, Texas, to Lake Charles, Louisiana. One year later, in 2008, Hurricane Ike (category 2) made landfall near Galveston, Texas, approximately 100 km to the east of SBNWR, with a sustained wind speed over 176 km/h. It caused up to 5-m-high storm surges and widespread coastal flooding along the coasts of Texas, Louisiana, Mississippi, and Alabama.

Most recently, at midnight of August 25, 2017, Hurricane Harvey (category 4) made landfall on San Jose Island near Aransas Bay, Texas, approximately 150 km to the west of SBNWR (Fig. 1) (Blake and Zelinsky 2017). Three hours later, it made a second landfall at the Texas mainland. After the second landfall, Harvey rapidly weakened to a tropical cyclone on August 26. During the next two days, Harvey stalled inland, dropping very heavy rainfall. It reemerged into the Gulf of Mexico on August 28 and then traveled east close to the Texas shoreline before making a third landfall in Louisiana, resulting in more record-breaking rainfall. Over a 4-day period, Harvey brought over 1000 mm of rain to many areas in south-central Texas, with a maximum precipitation of 1539 mm. Harvey was

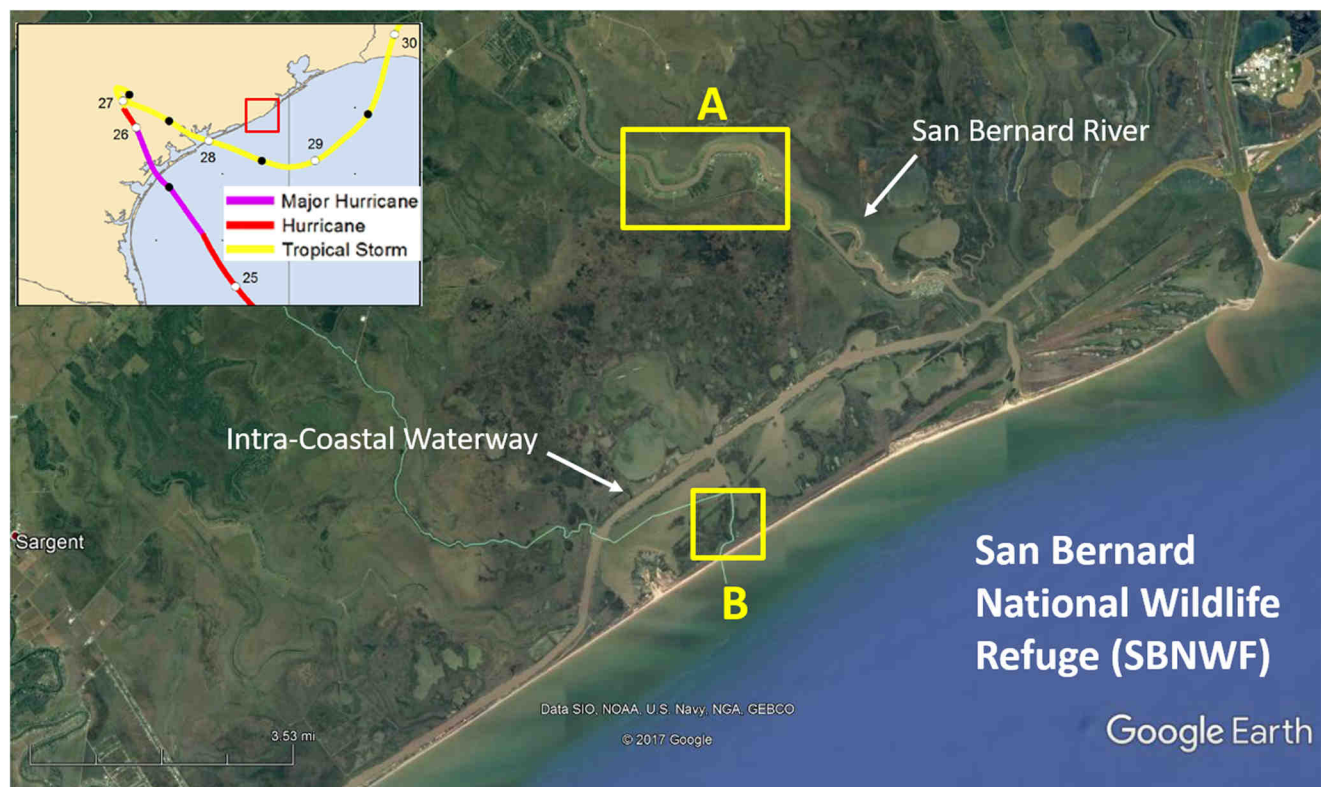


**Fig. 1** Map showing two focal areas of investigation (yellow boxes) within the San Bernard National Wildlife Refuge (SBNWR). Area A is where sediment cores were taken; area B is where surface samples were

collected. Inset map shows track of Hurricane Harvey (colors showing intensities) and location of SBNWR (red box)

the rainiest storm ever to make landfall in the United States, and it caused unprecedented flooding to east-central Texas. It caused 107 casualties in storm-related incidents and inflicted \$125 billion in damages (Blake and Zelinsky 2017).

## Methods

### Study Site

The SBNWR, established in 1968, is a  $\sim 185$  km $^2$  wildlife conservation area located along the coast of east-central Texas. It is  $\sim 65$  km west of Galveston, bordered to the east by the San Bernard River, to the south by the Gulf of Mexico, and to the west by Cedar Lake Creek, which forms the border between Brazoria and Matagorda counties. Historically, coastal zones along the east-central Texas coast have a distinct vegetation zonation consisting of the following three vegetation types: salt marsh along the shorelines, coastal prairies behind the salt marsh, and bottomland hardwood forest further inland (FWS 2010). Currently, because of the water management effort started in the late 1980s (Rachel 2018), the SBNWR maintains its historical zonation pattern. The refuge consists of low sand barriers about 1 m above mean sea level bordering bay estuaries that sustain massive oyster beds. At the north side of the bay, salinity is diluted by rainfall and freshwater runoff from the San Bernard River and the landscape slowly transforms from salt marsh into coastal prairie with many shallow water ponds. The coastal prairies and bottomland hardwood forests are in the floodplain of the Brazos River, Colorado River, and, in particular, the San Bernard River. The San Bernard River begins near Southwest Austin County and flows southwesterly for  $\sim 190$  km into the Gulf of Mexico (TPWD 2018). Our main sampling site ( $28^{\circ}53'02.4''$  N,  $95^{\circ}28'37.9''$  W) is located in the coastal prairie near the San Bernard River at approximately 10 km upstream from the Gulf of Mexico (Fig. 1). The San Bernard River was one of many rivers in the area that experienced overbank flooding in the days following the landfall of Hurricane Harvey, when record rainfalls occurred throughout the region (Fig. 2c).

### Field Sampling

Two field trips were conducted to retrieve short cores from SBNWR to study the distribution of the Hurricane Harvey storm deposit in order to assess the mode of deposition in relation to the contribution of fluvial versus marine processes in coastal flooding. In the first trip conducted in October 2017, about two months after the Harvey event, seven short cores, each  $< 30$  cm long, were collected along two transects to the south of the “big bend” of the San Bernard River, where satellite images taken immediately after Harvey revealed extensive overbank flooding by the meandering river (Fig. 2a).

Transect A ( $28^{\circ}53'48.12''$  N,  $95^{\circ}29'44.99''$  W), about 100 m long running away from State Highway 2918, consists of three short cores (SBW 20, 21, 22) (Fig. 2c). Transect B ( $28^{\circ}53'44.63''$  N,  $95^{\circ}31'15.35''$  W), also about 100 m long and consisting of four short cores (SBW 23, 24, 25, 26), was situated about 2 km west of transect A (Fig. 2b). Both transects were about 7 km from the Gulf of Mexico coast but only approximately 0.5 km from the nearest bank of the San Bernard River, and the elevation of the area is  $\sim 0.7$  m. Cores were taken variously by means of a Russian peat borer (SBW 20), 4-cm-diameter aluminum drainage pipe (SBW 21–24 and 26), and vibra-corer (core SBW 25). On another trip conducted in December 2017, a short core (SBW 209) ( $28^{\circ}53'49.08''$  N,  $95^{\circ}29'44.52''$  W) was collected very close to SBW 20 along transect A (Fig. 2c). In addition, another short core (SBW 202) ( $28^{\circ}54'9.60''$  N,  $95^{\circ}30'17.76''$  W) was retrieved from the natural levee only about 50 m from the southern bank of the San Bernard River. These cores were collected to replicate and verify the results obtained from earlier cores.

To provide baseline data to document the spatial variations of elemental chemistry in various coastal microenvironments, we collected 17 surface samples (SBSS 1–17) along a  $\sim 300$  m transect from the intertidal zone (SBSS 1–4) across sand dunes (SBSS 5–8) to backbarrier mudflat (SBSS 9–12) and saltmarshes (SBSS 13–17) in the coastal areas of the SBNWR (Fig. 3). The surface samples were retrieved by collecting the top 5 cm of sediments with a small shovel, and the chemical elemental data were to be used as a reference for interpreting the down-core variations in elemental chemistry measured by the XRF technique. The location of each coring and surface-sampling site was recorded by GPS.

Observations were made during field work to determine the depth of inundation during the Harvey-induced coastal flooding. Based on the height of the water marks and flood debris attached to plants, it was determined that the flood water was  $\sim 85$  cm deep along transect A (Fig. 4). All surface samples and cores were photographed in the field and have been stored in a cold room at 4 °C at the Global Change and Coastal Paleoecology Laboratory at Louisiana State University.

### Laboratory Analyses

In the laboratory, all cores were photographed again after unwrapping or splitting open longitudinally with a table saw and were described stratigraphically using the Munsell Color Chart. Cores 20, 21, and 22 from transect A and all cores from transect B were subjected to loss-on-ignition (LOI) and X-ray fluorescence (XRF) analyses. Cores 202 and 209 were only visually inspected, described, and photographed but were not analyzed by these techniques because these supplementary cores were only used to verify the sediment stratigraphies of cores obtained from transect A. A handheld Olympus Innov-X DELTA Premium XRF analyzer was used in this study. XRF

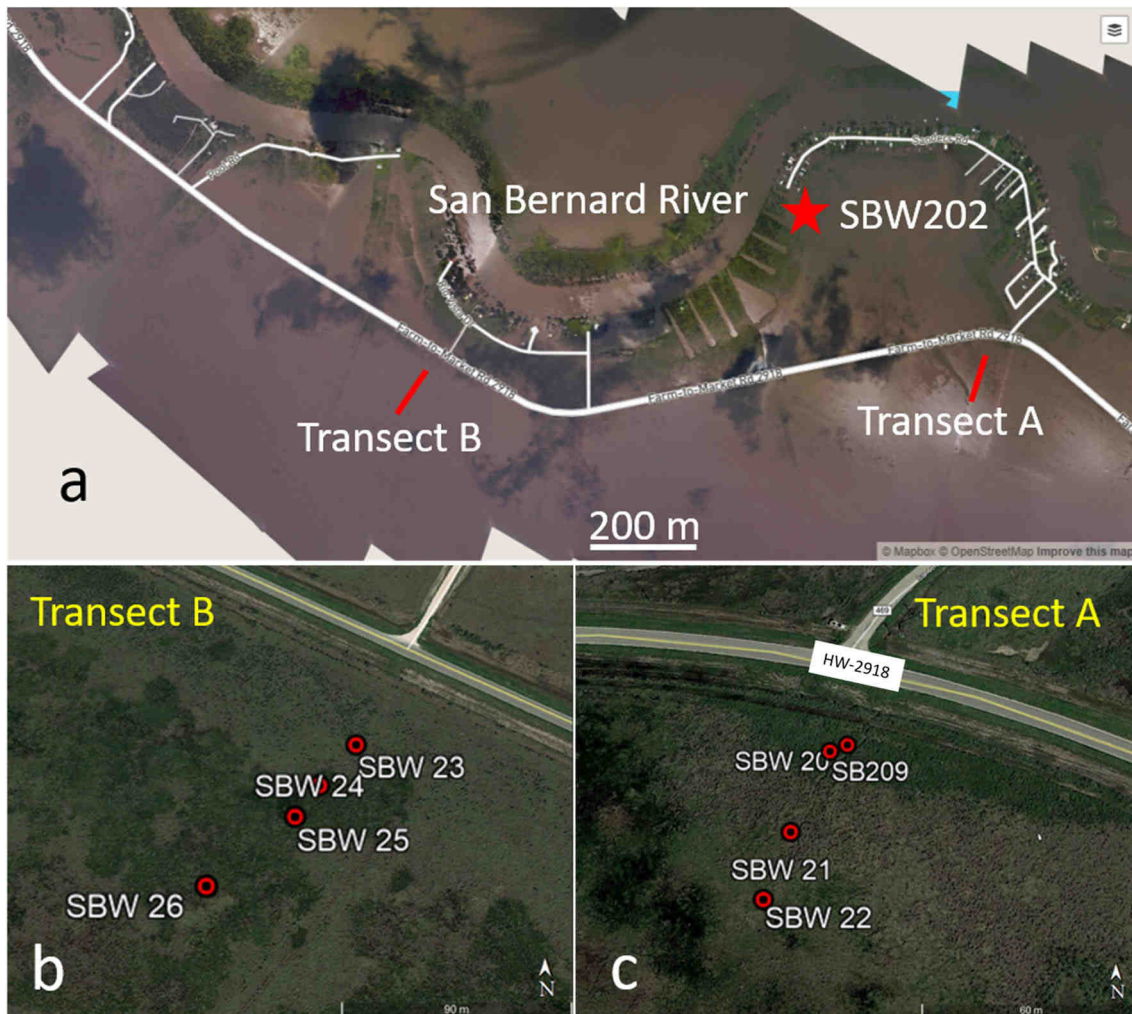


**Fig. 2** (a) Focal area A by the side of the San Bernard River showing overbank flooding during the Harvey event. Red star shows location of core 202. Red lines denote transects A and B. (b) Location of cores 23–28 along transect B. (c) Location of cores 209 and 20–22 along transect A

is a non-destructive analytical technique used to determine the elemental composition of materials. When a solid or liquid sample is excited by a primary X-ray source, elements present in a sample produce a fluorescent X-ray that is unique for that specific element. An XRF analyzer measures this energy and analyzes groups of elements simultaneously in order to rapidly determine those elements present in the sample and their relative concentrations. A total of 15 elements were detected in our samples, but 6 of them were present only in trace amounts with no systematic changes. Therefore, only 9 common elements (S, Cl, Ca, Sr, Zr, Br, K, Ti, and Fe) and the chlorine/bromine (Cl/Br) ratio are presented in this study. Previous studies have successfully used XRF analysis to identify marine indicators in coastal sediments (e.g., Cl, Ca, Sr, and Zr) (Ramrez-Herrera et al. 2012; Liu et al. 2014; McCloskey et al. 2018a, 2018b; Ercolani et al. 2015), as well as terrestrial runoffs (e.g., Fe, Ti, and K) in sedimentary records (Haug et al. 2001; You 2008; van Soelen et al. 2012). In particular, the Cl/Br ratio has been used as a marine indicator in

sediment-stratigraphic studies in coastal and estuarine environments (Liu et al. 2014; McCloskey et al. 2018a, 2018b; Yao et al. 2018). The elemental concentrations are reported in parts per million (ppm), and the Cl/Br ratio was generated based on the concentration counts (ppm). Loss-on-ignition (LOI) analyses were used to reveal the % wet weight for water and % dry weight for organics and carbonates throughout the cores and surface samples. The XRF and LOI analyses were performed at 1 cm interval for these cores, and laboratory procedures followed those described in Yao et al. (2015, 2018) and Yao and Liu (2017, 2018).

### Hydrological Data

To put the magnitude of the Harvey flood event in the historical context, we analyzed the hydrological data for the San Bernard River for a 28-year period from 1990 to 2017. For daily discharge ( $Q_d$  in cm) and daily sediment load ( $DSL$  in ton/day) records, we used the gauging station at Boling about 90 km

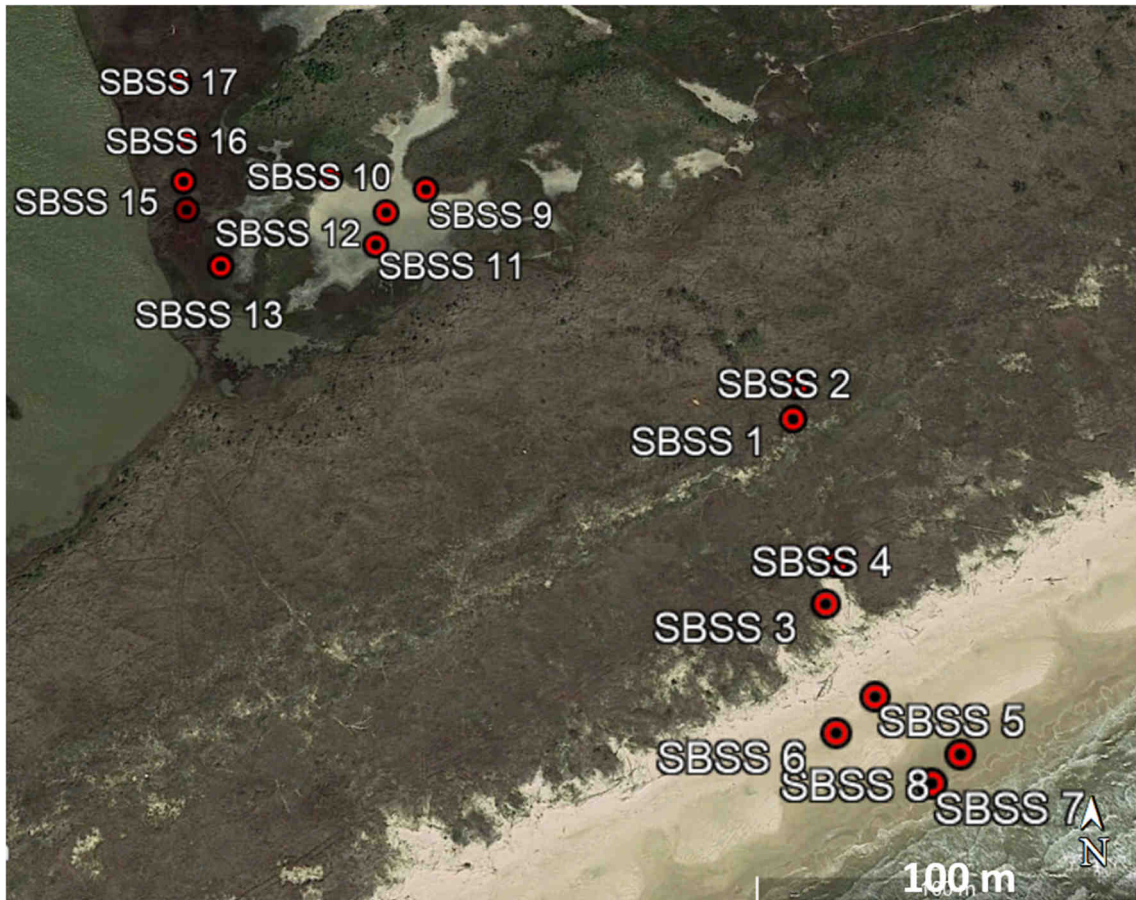


**Fig. 3** Focal area B by the coast of San Bernard NWR showing location of the 17 surface samples

north of SBNWR (USGS ID 08117500) (USGS 2018). Twenty-eight years of  $Q_d$  data (1990–2017) were collected from Boling to document the long-term discharge record of the San Bernard River; in addition, hourly discharge records ( $Q_{hr}$ ) were compiled from real-time discharge data (at 15-min intervals) at Boling, from August 26 to September 7, 2017, to analyze the hourly fluctuations in river flooding during the passage of Hurricane Harvey. The daily sediment loads ( $DSL$ ) in the San Bernard River at Boling during Hurricane Harvey were calculated according to the following formula:  $DSL = Q_d \times SSC \times 0.0864$ . Calculation for the daily suspended loads ( $SSL_d$ ) is described in Joshi and Xu (Joshi and Xu 2015; Joshi and Xu 2017). Storm surge data were retrieved from the SURGEDAT database (<http://surge.srcc.lsu.edu>).

## Results

### Long-Term Flow Conditions in the San Bernard River

The average daily discharge ( $Q_d$ ) at Boling along the San Bernard River is  $\sim 17$  cm from 1990 to 2017 (Fig. 5a). Over the 28-year period,  $Q_d$  for the river exceeded 100 cm for only

390 days, remained between 10 and 100 cm for 2275 days, and was less than 10 cm for the remaining 7563 days (calculated based on Fig. 5a). Among those high discharge events ( $Q_d > 100$  cm), the highest level in  $Q_d$  was recorded during Harvey, when  $Q_d$  increased from 289 cm (August 27, 2017) to 1405 cm (September 1, 2017) and then decreased back to 125 cm (September 7, 2017) (Fig. 5). The second highest level in  $Q_d$  over the 28-year period was in October 1998, when  $Q_d$  reached 886 cm. A few other notable high discharge events for San Bernard River at Boling occurred in June 1993 (431 cm), October 1994 (the Great Flood of Houston, 549 cm), September 2001 (357 cm), November 2002 (498 cm), and November 2004 (442 cm). The hourly discharge ( $Q_{hr}$ ) at Boling in the San Bernard River recorded two peaks during the landfall of Hurricane Harvey. The first peak was 1184 cm at 2 pm on August 30. The second and the highest recorded  $Q_{hr}$  at Boling was 1511 cm at 12 am on September 1, 2017 (Fig. 5b).

### Suspended Sediment Load in the San Bernard River During Harvey

The San Bernard River had an average daily suspended sediment load ( $SSL_d$ ) of 848 ton/day during August and



**Fig. 4** Mud and wrack caught on the plants showing the maximum height (red arrow by the meter stick:  $\sim 0.85$  m) of the flood water near core 20

September 2017 (USGS ID 08117500) (USGS 2018). The  $SSL_d$  for the San Bernard River varied between 0.42 and 104 ton/day from August 1 to 25, 2017 (before Harvey); between 739 and 7575 ton/day from August 26 to September 7, 2017 (during Harvey); and between 11 and 579 ton/day from September 8 to 30, 2017 (post Harvey) (Fig. 6). It should be noted that even during the peak of the Harvey-induced flood event on September 1, 2017, the maximum  $Q_d$  (1405 cm) and  $SSL_d$  (7575 tons/day) for the San Bernard River were only a tiny fraction of the corresponding maxima for adjacent Trinity River (3510 cm; 128,657 tons/day) and Brazos River (3360 cm; 1,146,725 tons/day) (Sanjeev Joshi, unpublished data) (Fig. 6). This is due to the fact that the drainage basin of the San Bernard River covers a much smaller area than the latter two neighboring rivers.

### Storm Surge Data at SBNWR

Tidal gauge data from Sargent, Freeport, and San Luis Pass, the three nearest stations relative to our study area (SURGEDAT 2018), show that the height of storm surges reached up to  $\sim 1$  m at Sargent on August 29 (Fig. 7). All three sites recorded two peak storm surges on August 26 and

29. The heights of the two peak storm surges are  $\sim 0.9$  m and  $\sim 0.92$  m at San Luis Pass,  $\sim 0.65$  m and  $\sim 0.4$  m at Freeport, and  $\sim 0.7$  m and  $\sim 1$  m at Sargent, respectively.

### Storm Deposits

Of all 9 cores collected for this study, only three (SBW 202, 20, 209) contain a distinct storm deposit identifiable upon visual inspection in the field or in the laboratory. Core SBW 202 was taken at the foot of the natural levee only 50 m from the San Bernard River (Fig. 2). The flood deposit occurs in the form of a 9-cm-thick light gray, rootless, inorganic mud resting on brownish-gray organic rooted mud representing the pre-flood marsh surface (Fig. 8). The presence of this flood deposit here is not surprising due to this site's proximity to the river. A similar light gray inorganic mud layer was found at the top of core SBW 209 in transect A, located about 50 m into the marsh from Highway 2918. This 4-cm-thick rootless flood deposit overlies an organic-rich marsh deposit containing many plant roots (Fig. 8). Core SBW 20, located very close to SBW 209, also contains a distinct storm deposit at the top. This tilted layer, ranging from  $\sim 5$  to 10 cm in thickness from one side to the other, consists of two light-color inorganic units separated by a thin organic detritus layer in the middle (Fig. 8). The marsh surface in that part of transect A was hummocky with a micro-topography of mounds and depressions formed by clumps of bunch grasses, which may contribute to the uneven thickness of the storm deposit at the coring site.

### Lithology and Chemical Stratigraphy

The other cores taken from transect A (SBW 21–22) and transect B (SBW 23, 24, 25, 26) do not contain a distinct storm deposit at the top, but they have similar stratigraphic profiles. All cores consist of gray rooted sediment at the base. These organic rooted sediments have relatively low water (<30%) and organic matter (<5%) contents, and the elemental concentrations of all elements are relatively consistent in most intervals throughout the rooted sediments (Fig. 9). Most cores show a slight increase in organic matter content near the top, while a few cores (SBW 20, 22, 24) contain a peak in organic matter at 2–4 cm from the top (Fig. 9). XRF analysis detects a rise in Cl/Br ratio at the  $\sim 3$ –10 cm level, followed by a decline at the top (Fig. 9). This rise in Cl/Br ratio is more prominent in some cores (SBW 20, 21, 22, 25, 26) but subtler or indistinct in others (SBW 23, 24). In core SBW 20, a prominent peak in Cl/Br ratio occurs at the base of the storm deposit, but, in other cores (e.g., SBW 22, 25, 26), a peak seems to be present even though no distinct storm deposit is present.

Despite their overall similarities, LOI and XRF profiles also exhibit different characteristics between cores along transects A and B. The water (25–50% vs. <20%) and organic

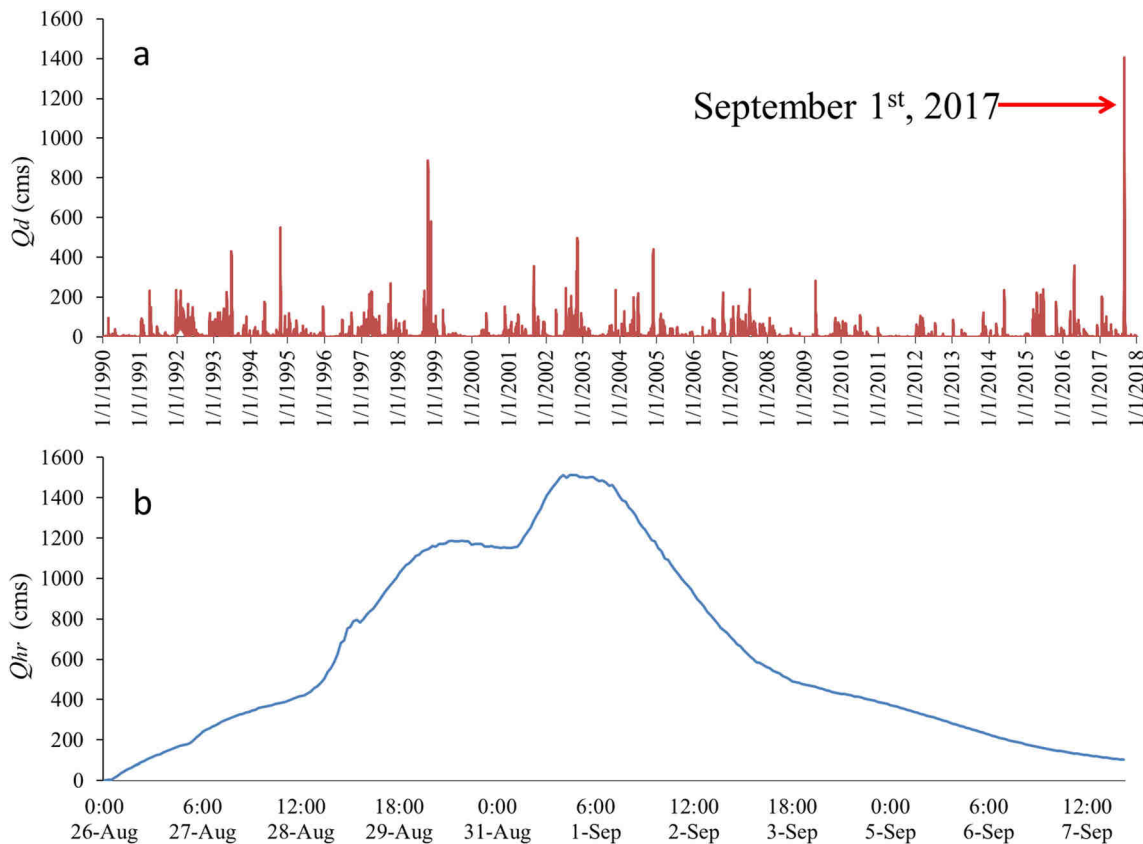


**Fig. 5** (a) Daily discharge ( $Q_d$ ) for the San Bernard at Boling from January 1, 1990, to December 31, 2017. (b) Hourly discharge ( $Q_{hr}$ ) for the San Bernard River at Boling during Hurricane Harvey from August 25 to September 7, 2017

matter (10–20% vs. 5–10%) contents in cores from transect A are generally higher than those in cores from transect B, particularly at the top portion of the cores, but the concentrations of Ca are significantly lower in cores from transect A (<2000 ppm) than cores from transect B (3000–5000 ppm).

### Surface Samples

The 17 surface samples taken from 4 different environmental settings exhibit distinct sedimentological and chemical gradients (Fig. 10). Samples SBSS-1 to SBSS-4, taken from the

beach and intertidal zone, contain very low contents of water, organics, and carbonates and high concentrations of Ca, resembling typical marine-originated sediments (Yao and Liu 2018; Yao et al. 2018). Moving inland, sand dune samples SBSS-5 to SBSS-8 have sedimentological and chemical characteristics broadly similar to the intertidal group, except for higher Zr contents and the exponentially high Cl/Br ratios due to the negligible amounts of Br in these samples. Samples SBSS-9 to SBSS-12, taken from the backbarrier mudflat, show very different signals than the previous two groups.

**Fig. 6** Daily suspended sediment load ( $SSL_d$ ) for the San Bernard (Boling), Brazos (Richmond), and Trinity (Liberty) Rivers during August and September 2017. Note: Hurricane Harvey occurred from 8/25/2017 to 9/5/2017

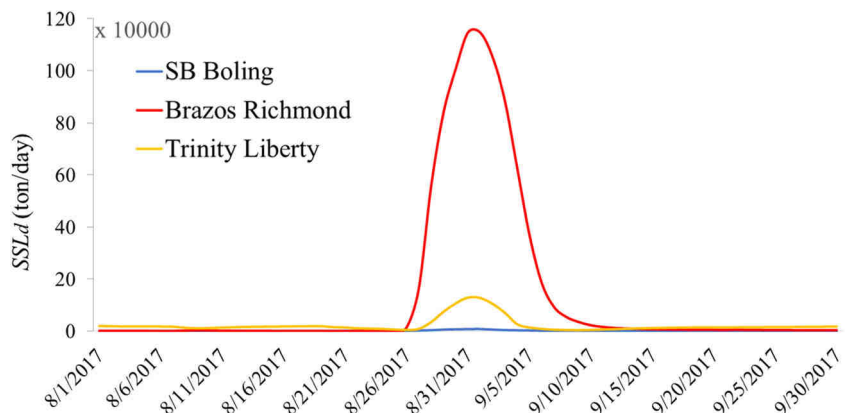
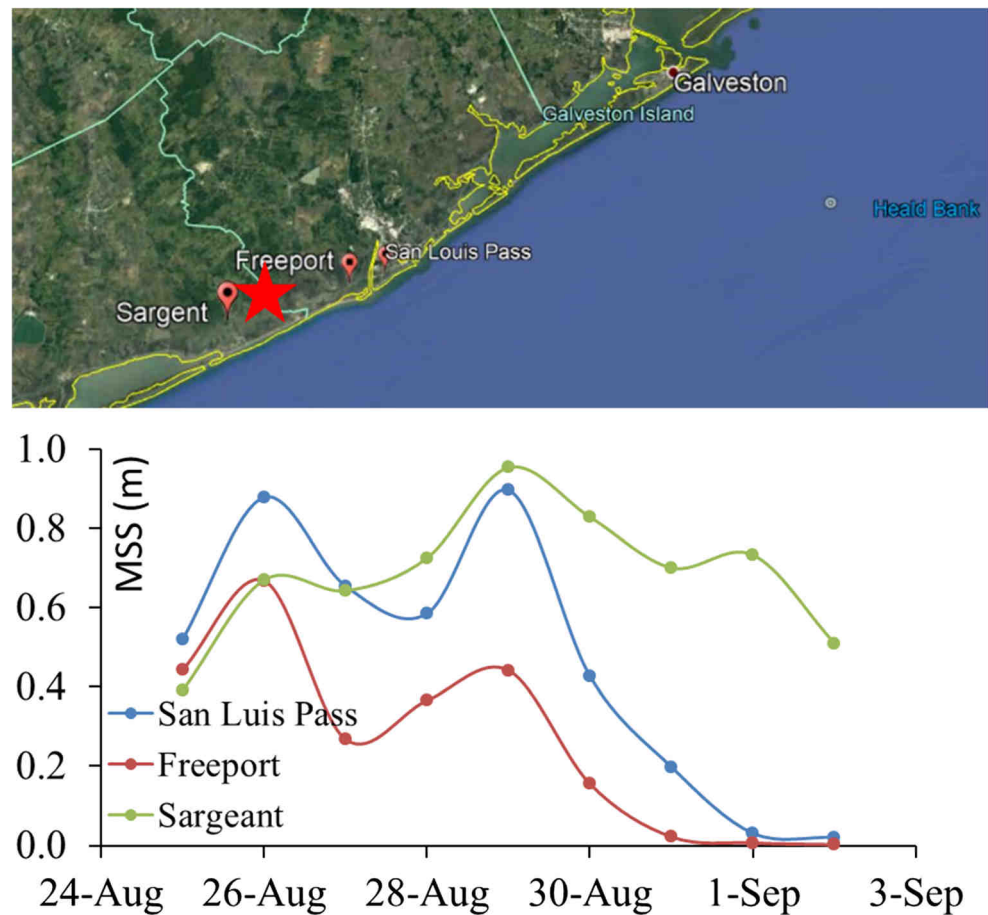


**Fig. 7** Maximum storm surge (MSS) at locations nearest to our sampling sites (red star) in the SBWR (August 25–September 1, 2017)



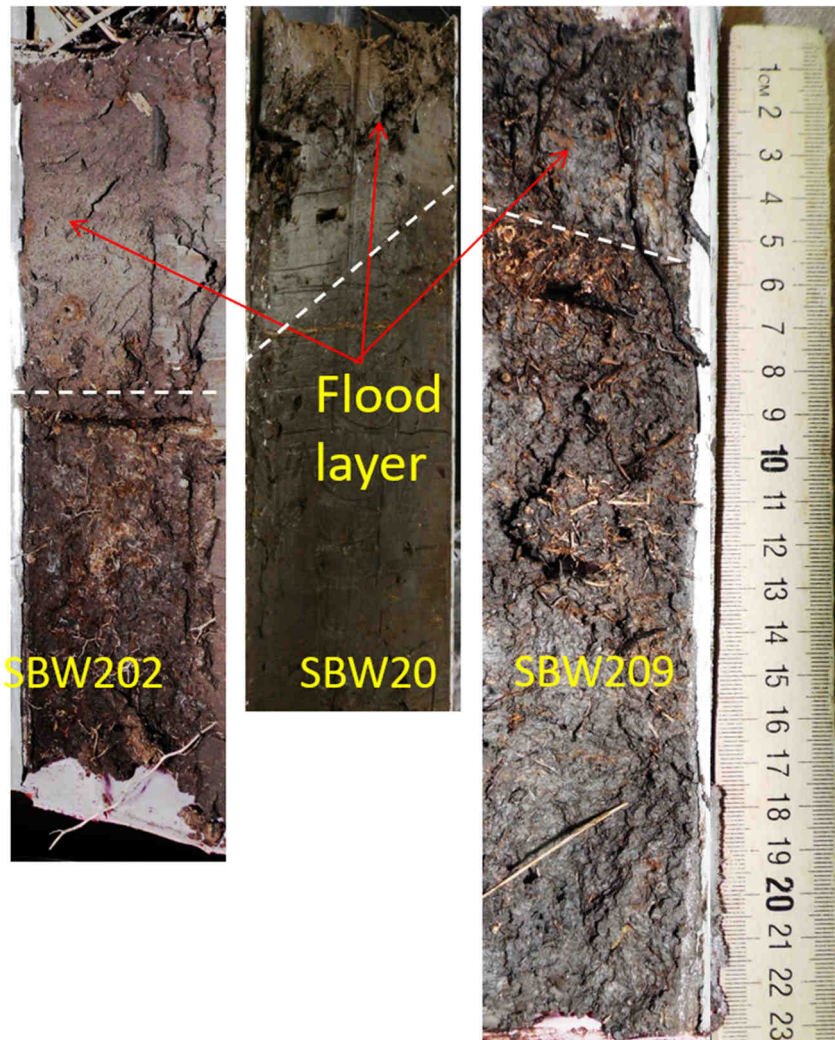
Contents of water, organics, and especially carbonates increase significantly in this group. XRF results also indicate a significant increase in both Cl and Br and slight increase in K, Ti, and Fe, typical indicators for terrestrial originated sediments (Yao et al. 2015; Yao and Liu 2017). The Cl/Br ratio, however, is much lower than that in the beach and dunes groups that are closer to the marine environment. Samples SBSS-13 to SBSS-17, taken from the saltmarsh behind the mudflat, are marked by a significant increase in the water content, decrease in marine indicators (Ca, Sr, and Zr), and gradual increase in the terrestrial indicators (K, Ti, and Fe). Most remarkably, the Cl/Br ratio is the lowest of the four coastal groups as this saltmarsh group is located farthest away from direct marine influence. To reveal the differences between the coastal prairie/floodplain deposits at our coring sites and surface samples from the coastal area, we included the LOI and XRF results of the top layers of core SBW 20–26 at the bottom of Fig. 10. In comparison, the core top samples contain much higher contents of organic matter and terrestrial elements (K, Ti, Fe), but the Cl/Br ratio is the lowest among all the groups.

## Discussion

### Sedimentary Signature of Hurricane Harvey

Satellite images clearly show that our coring sites were inundated by floodwaters after Hurricane Harvey's landfall (Fig. 2a). Field observations based on water marks and wrack lines suggest that the floodwater was approximately 85 cm deep near core SBW 20 along transect A (Fig. 4). The storm surge data show two peaks on August 26 and 29, with the first peak reaching 0.65–0.9 m and the second peak reaching 0.4–1.0 m in height (Fig. 7). Although there is no evidence that the sand dunes were overtapped or breached by the storm surge, it is likely that during the landfall of Hurricane Harvey, a large quantity of seawater was introduced into the bays and estuaries behind the sand dunes at SBNWR (Fig. 1). The Intra-Coastal Waterway may also serve as a conduit to allow the seawater to spread onto the marshes and shallow ponds behind it. Thus, it is likely that our coring sites along the two transects, which were at ~ 0.7 m elevation, were affected by seawater during the first and perhaps also the second storm surge during the landfall. However, the

**Fig. 8** Photos of distinct flood layers (above the white dash lines) at the top of core SBW 202, 20, and 209



wave energy of the storm surge waters would probably have been significantly attenuated due to the protection by the coastal sand dunes, and the storm surge waters probably did not carry much coarse marine sediments as they would have been trapped or filtered by the shallow ponds and marsh vegetation before they could reach our coring sites. This explains the lack of a distinct layer of storm surge or washover sediments at our coring sites. Despite this lack of sedimentary evidence for storm surge deposition, the inundation by seawater did leave a geochemical signal at our study sites in the form of an elevated Cl/Br ratio near the top of the sediment cores (Fig. 9). Our surface sample study has shown that the Cl/Br ratios are higher in intertidal and sand dune environments that are closer to the Gulf of Mexico than in mudflat and saltmarsh environments that are less exposed to marine influences, whereas our coring sites situated farthest away from the coast have the lowest Cl/Br ratios (Fig. 10). Therefore, these surface sample data confirm results from previous studies that the Cl/Br

ratio can be used as a salinity indicator and, as a corollary, evidence of marine intrusion into lower-salinity environments (Alcalá and Custodio 2004; Liu et al. 2014; McCloskey et al. 2018a, 2018b; Yao et al. 2018). Stratigraphically, the peaks in Cl/Br ratio are more prominent or thicker in some cores but are more subtle or thinner in others, and it may occur near the top in some cores and deeper (down to 5–12 cm) in others. The deeper occurrence may be due to the downward percolation of the storm surge seawater through the root zone of the marsh plants.

Heavy precipitation brought on by Hurricane Harvey caused extensive flooding of the San Bernard River. Our hydrological data show that the discharge and suspended load of the San Bernard River peaked on September 1, three days after the second storm surge peak (Fig. 5). The discharge peak also lasted for nearly a week before it returned to normal level (Fig. 5b). Thus, there is no doubt that freshwater flooding from the San Bernard River is the predominant cause of the inundation at the study sites. Evidence of the overbank

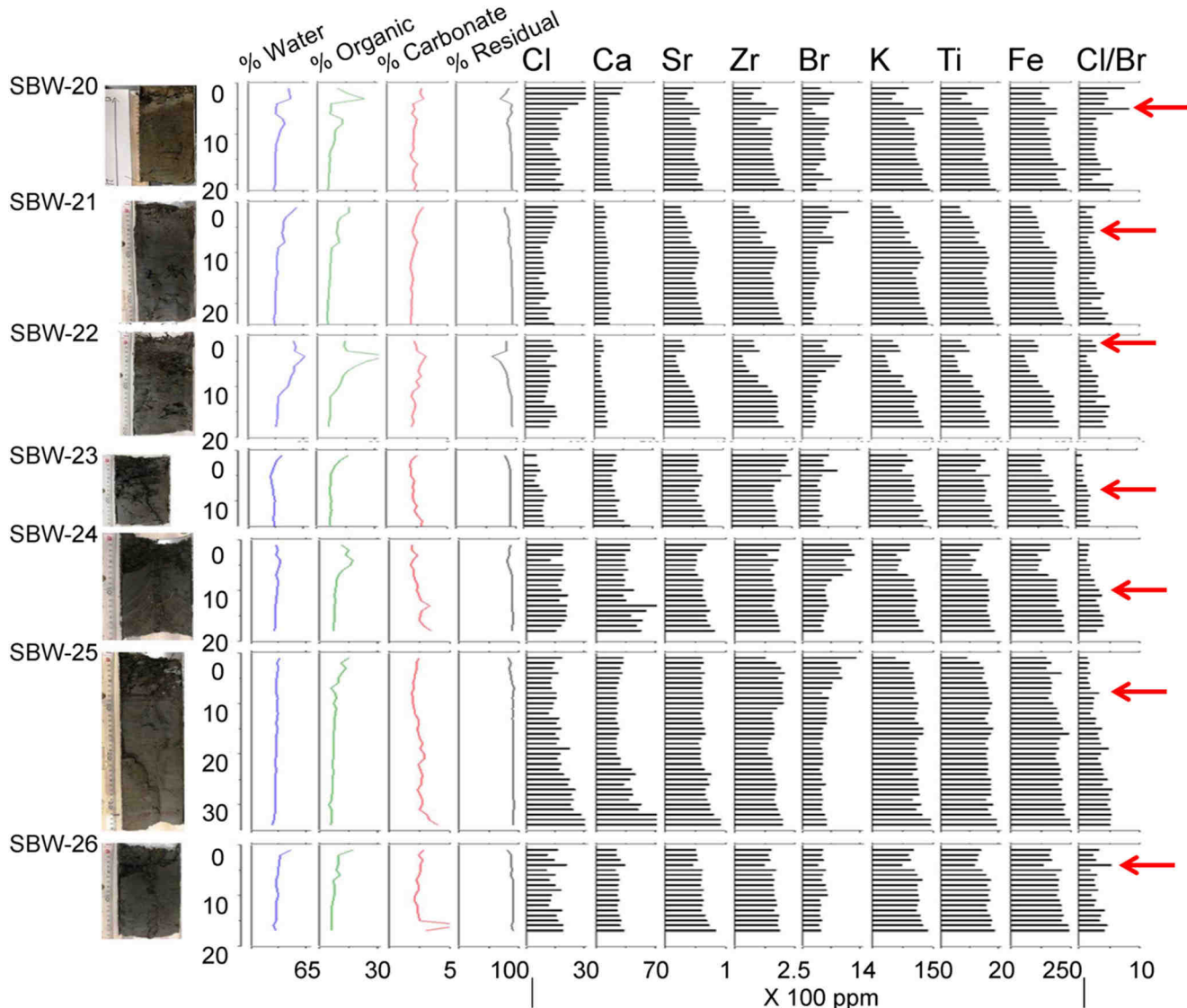


**Fig. 9** From left to right, photograph, LOI, and XRF diagrams of core SBW-20A to SBW-26. The red arrows point to the rise in Cl/Br ratios

flooding is clearly registered in core SBW 202 collected on the natural levee only ~ 50 m from the river, which contains a 9-cm-thick flood deposit at the top. A 4–5-cm-thick flood deposit also occurs at the top of cores SBW 209 and 20 along transect A, about 0.5 km from the river. However, it is remarkable that most of the cores do not contain a distinct flood deposit at the top that can be attributable to the Harvey flood event. The absence of distinct sedimentary evidence may be explained by our hydrological data which show that, in comparison with the larger neighboring Brazos and Trinity Rivers, the San Bernard has a much smaller discharge and does not carry as much suspended sediment load. In addition, the fresh fluvial deposit attributed to the Harvey-generated flood—even if present—may not be easily distinguishable from the underlying fluvial sediments contained in the core because the coring sites are located on a floodplain which was built up largely

by alluvium deposited by past flood events from the same river (Falcini et al. 2012).

### Overview of the Regional Paleotempestological Studies

Many proxy-based storm records have been published from study sites along the Gulf Coast in recent years (e.g., Liu et al. 2008; Williams 2010, 2012; Williams and Flanagan 2009; Lane et al. 2011; Wallace and Anderson 2010; Wallace et al. 2014; McCloskey et al. 2018a, 2018b; Das et al. 2013; Ercolani et al. 2015; Wang et al. 2019). Most of these studies have focused on the detection of storm deposits created by overwash processes in backbarrier lakes and estuarine marshes. Washover deposits are typically sandy, as their materials are typically derived from the beach and dunes that lie

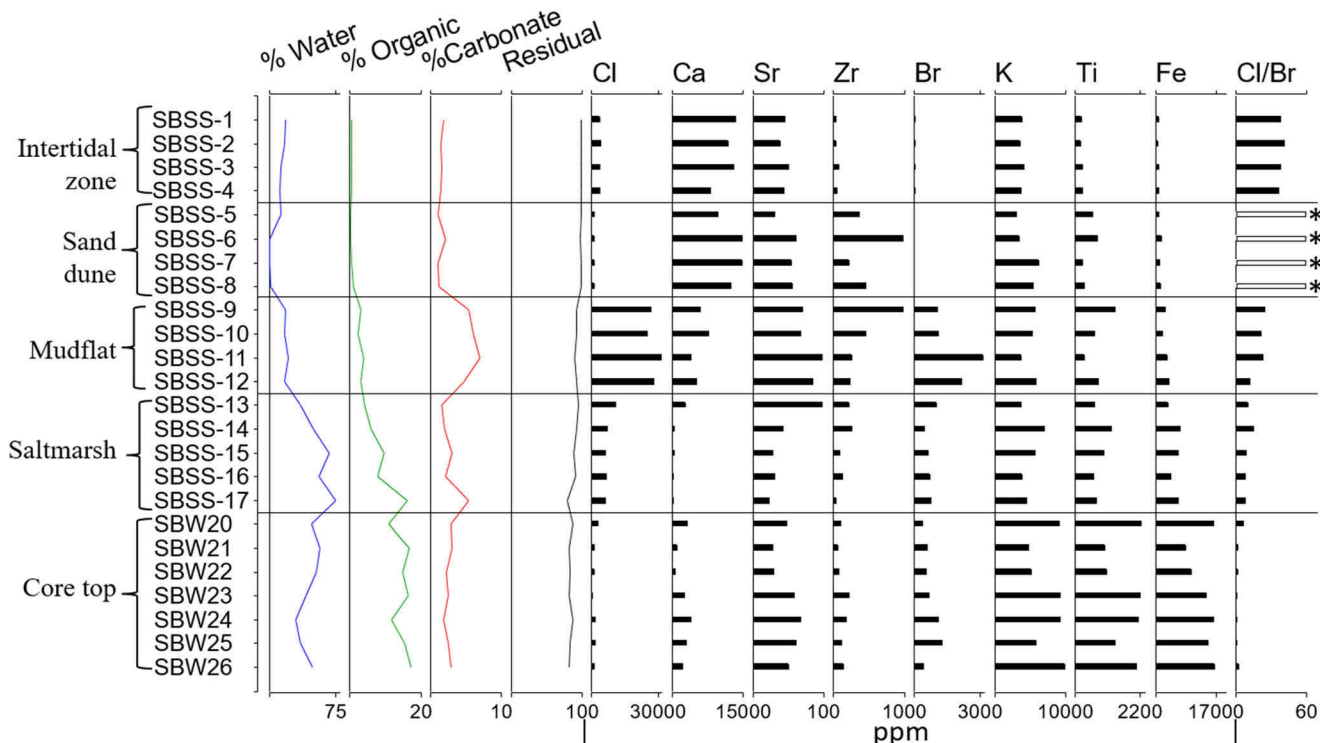


**Fig. 10** LOI and XRF diagrams of surface samples SBSS-1 to SBSS-17 and top layer of core SBW20 to SBW26 (\* Samples with exceptionally high Cl/Br ratios)

in front of the coring sites, as well as marine sediments transported by waves and currents under high-energy conditions (Liu and Fearn 1993, 2000; Liu 2004; Liu et al. 2008, 2011, 2014; Breyg et al. 2018). Thus, washover sediments can be identified by a distinct drop in water and organic matter contents in the LOI results and an increase in the Cl/Br ratio in the XRF results (Liu 2004; Liu et al. 2014; Yao et al. 2018; Ryu et al. 2018). However, the storm deposition generated by Hurricane Harvey in SBNWR poses a special challenge to paleotempestology, as it probably involves an initial phase of seawater intrusion followed by an extended phase of fluvial sedimentation due to freshwater flooding from an adjacent river. Although a lack of overwash processes during the initial storm surge phase caused the absence of a distinct sand layer in all of the coring sites, the seawater intrusion can still be detected by a peak in the Cl/Br ratio in the geochemical profile of most sediment cores.

For paleotempestological study, it is clear that not all hurricanes that come near the study area will be recorded. Many factors are required for the preservation of the storm deposits, such as ideal beach barrier dimensions, short site-to-sea distance, and stable sedimentary environment of the study site, among others (Liu 2004). In addition, many paleotempestological studies have indicated that most sites are not sensitive enough to record hurricane landfalls beyond the immediate vicinity, and only intense hurricanes (category 3 and above) will be recorded (Liu 2004; Donnelly and Webb III 2004; Elsner et al. 2008). However, as some sites across the Gulf record different

threshold events as well as varying background sedimentation rates, a careful consideration of these factors must occur for site comparison (Wallace et al. 2014). The only way to bridge the gaps between the existing hurricane records is to conduct paleotempestological studies in more locations throughout the western Atlantic Basin, so that we can put all the records in the regional context to better determine the long-term hurricane dynamics. In this study, we demonstrated that XRF analysis, in particular using the Cl/Br ratio as an indicator, can be used to identify storm events in the sedimentary record in the absence of overwash processes. Although site-sensitivity remains an issue, this study shows the potential to obtain storm records in a wider range of geomorphological conditions, in particular sand-limited coastal systems where traditional sedimentological proxies (i.e., washover sand layers) are absent or ineffective. This methodological advancement allows more coastal and estuarine locations across the North Atlantic to become amenable to paleotempestological studies, thereby enabling more proxy records to be produced from otherwise sub-optimal sites, such as the sand-limited coastal prairies along the Texas coastlines. One question that warrants further investigation concerns the preservation potential of the geochemical signals in the sediment stratigraphy. The sediment coring and the XRF analysis in this study were conducted within four months after the Harvey storm event. A follow-up coring campaign would be useful to determine if the geochemical signals especially the Cl/Br ratio are still preserved in the sediment profiles at the same sites along the study transects after several years.

## Conclusions

This study investigated the depositional process associated with Hurricane Harvey from wetland sites near the San Bernard River at the SBNWR, Texas. Our hydrological data indicate that Hurricane Harvey caused the largest flooding within SBNWR over the last 28 years, and freshwater flooding from the San Bernard River is the predominant cause of the inundation at the study sites. Due to the lack of overwash processes during the initial storm surge phase, a distinct sand layer is lacking in all of the coring sites, but the intrusion of seawater can still be detected by a peak in the Cl/Br ratio in the chemical stratigraphy of most sediment cores. The ensuing phase of freshwater flooding and fluvial sedimentation is represented by a distinct flood deposit in only a few sites, but absent or not clearly identifiable in most cores. The elusiveness of the fluvial flood deposit in SBNWR suggests that it is thin and not evenly distributed, even at our coring sites that are only 0.5 km away from the San Bernard River. The relatively low discharge and suspended sediment load of the San Bernard River, which were spread out over a large coastal prairie/marsh on a floodplain, probably account for the thin and uneven distribution of the flood deposit. The similarity between the fluvial deposit generated by Harvey's flood and the underlying sediment deposited by previous floods on the floodplain may also contribute to the difficulty in the identification of Harvey's flood deposit. More work needs to be done to confirm the results from this pilot study of Hurricane Harvey's sedimentation patterns and processes.

**Acknowledgments** This research was supported by a grant from the National Science Foundation (NSF RAPID Grant No. EAR-1803035). We are grateful to all the staff members of the San Bernard National Wildlife Refuge for their logistical support. We also thank Lance Riedlinger and Gabrien Panteria for their assistance in the laboratory.

## References

Alcalá, F. J. and Custodio, E., 2004. Use of the Cl/Br ratio as a tracer to identify the origin of salinity in some coastal aquifers of Spain. In: Groundwater and saltwater intrusion: Selected papers from the 18th saltwater intrusion meeting (ed. by Araguás, L., Custodio, E. & Manzano, M), 481–498. Publicaciones del Instituto Geológico y Minero de España.

Bianchette, T.A., T.A. McCloskey, and K.-B. Liu. 2016. Re-evaluating the geological evidence for Late Holocene marine incursion events along the Guerrero Seismic Gap on the Pacific Coast of Mexico. *PLoS One* 11 (8): e0161568. <https://doi.org/10.1371/journal.pone.0161568>.

Blake, E. S. and Zelinsky, D. A., 2017. National hurricane center tropical cyclone report—Hurricane Harvey, website: [https://www.nhc.noaa.gov/data/tcr/AL092017\\_Harvey.pdf](https://www.nhc.noaa.gov/data/tcr/AL092017_Harvey.pdf)

Bregy, J.C., D.J. Wallace, R.T. Minzoni, and V.J. Cruz. 2018. 2500-Year paleotempestological record of intense storms for the northern Gulf of Mexico, United States. *Marine Geology* 396: 26–42.

Das, O., Y. Wang, J. Donoghue, X. Xu, J. Coor, J. Elsner, and Y. Xu. 2013. Reconstruction of paleostorms and paleoenvironment using geochemical proxies archived in the sediments of two coastal lakes in northwest Florida. *Quaternary Science Reviews* 68: 142–153.

Donnelly, J.P., and T. Webb III. 2004. Back-barrier sedimentary records of intense hurricane landfalls in the northeastern United States. In *Hurricanes and typhoons: Past, present and future*, ed. R.J. Murnane and K.B. Liu, 58–95. New York: Columbia University Press.

Donnelly, J.P., and J. Woodruff. 2007. Intense hurricane activity over the past 5000 years controlled by El Niño and the West African Monsoon. *Nature* 44: 465–468.

Duan, N. 1983. Smearing estimate: A nonparametric retransformation method. *Journal of the American Statistical Association* 78 (383): 605–610.

Elsner, J.B., T.H. Jagger, and K.B. Liu. 2008. Comparison of hurricane return levels using historical and geological records. *Journal of Applied Meteorology and Climatology* 47 (2): 368–374.

Ercolani, C., J. Muller, J. Collins, M. Savarese, and L. Squicciara. 2015. Intense southwest Florida hurricane landfalls over the past 1000 years. *Quaternary Science Reviews* 126: 17–25.

Falcini, F., N.S. Khan, L. Macelloni, B.P. Horton, C.B. Lutken, K.L. McKee, R. Santolieri, S. Colella, C. Li, G. Volpe, and M. D'Emidio. 2012. Linking the historic 2011 Mississippi River flood to coastal wetland sedimentation. *Nature Geoscience* 5 (11): 803–807.

Gray, A.B., G.B. Pasternack, E.B. Watson, J.A. Warrick, and M.A. Goni. 2015. Effects of antecedent hydrologic conditions, time dependence, and climate cycles on the suspended sediment load of the Salinas River, California. *Journal of Hydrology* 525: 632–649.

Haug, G.H., K.A. Hughen, D.M. Sigman, L.C. Peterson, and U. Röhl. 2001. Southward migration of the intertropical convergence zone through the Holocene. *Science* 293 (5533): 1304–1308.

Joshi, S., and Y.J. Xu. 2015. Assessment of suspended sand availability under different flow conditions of the lowermost Mississippi River at Tarbert landing during 1973–2013. *Water* 7 (12): 7022–7044.

Joshi, S., and Y.J. Xu. 2017. Bedload and suspended load transport in the 140-km reach downstream of the Mississippi River avulsion to the Atchafalaya River. *Water* 9 (9): 716.

Khan, N.S., B.P. Horton, K.L. McKee, D. Jerolmack, F. Falcini, M.D. Enache, and C.H. Vane. 2013. Tracking sedimentation from the historic AD 2011 Mississippi River flood in the deltaic wetlands of Louisiana, USA. *Geology* 41 (4): 391–394.

Lane, P., J.P. Donnelly, J.D. Woodruff, and A.D. Hawkes. 2011. A decadally resolved paleohurricane record archived in the late Holocene sediments of a Florida sinkhole. *Marine Geology* 287 (1–4): 14–30.

Liu, K.B. 2004. In *Palaeotempestology: Principles, methods and examples from Gulf coast lake sediments*, ed. R. Murnane and K.B. Liu, 13–57. New York: Columbia University Press. Hurricanes and typhoons: Past, present and future

Liu, K.B., and M.L. Fearn. 1993. Lake-sediment record of late Holocene hurricane activities from coastal Alabama. *Geology* 21 (9): 793–796.

Liu, K.B., and M.L. Fearn. 2000. Reconstruction of prehistoric landfall frequencies of catastrophic hurricanes in northwestern Florida from lake sediment records. *Quaternary Research* 54 (2): 238–245.

Liu, K.B., H.Y. Lu, and C.M. Shen. 2008. A 1,200-year proxy record of hurricanes and fires from the Gulf of Mexico coast: Testing the hypothesis of hurricane-fire interactions. *Quaternary Research* 69 (1): 29–41.

Liu, K.B., C. Li, T.A. Bianchette, T.A. McCloskey, Q. Yao, and E. Weeks. 2011. Storm deposition in a coastal backbarrier lake in Louisiana caused by Hurricanes Gustav and Ike. *Journal of Coastal Research, SI* 64: 1866–1870.

Liu, K.B., T.A. McCloskey, S. Ortego, and K. Maiti. 2014. Sedimentary signature of Hurricane Isaac in a *Taxodium* swamp on the western margin of Lake Pontchartrain, Louisiana, USA. In *Proceedings of the International Association of Hydrological Sciences*, vol. 367, 421–428.

McCloskey, T.A., and K.-b. Liu. 2012. A sedimentary-based history of hurricane strikes on the southern Caribbean coast of Nicaragua. *Quaternary Research* 78 (3): 454–464.

McCloskey, T.A., and K.-B. Liu. 2013. A 7000-year record of paleohurricane activity from a coastal wetland in Belize. *The Holocene* 23: 276–289.

McCloskey, T.A., T.A. Bianchette, and K.B. Liu. 2015. Geological and sedimentological evidence of a large tsunami occurring ~1100 year BP from a small coastal lake along the Bay of La Paz in Baja California Sur, Mexico. *Journal of Marine Science and Engineering* 3 (4): 1544–1567.

McCloskey, T.A., C.G. Smith, K.B. Liu, M. Marot, and C. Haller. 2018a. How could a freshwater swamp produce a chemical signature characteristic of a saltmarsh? *ACS Earth and Space Chemistry* 2 (1): 9–20.

McCloskey, T.A., C.G. Smith, K.B. Liu, and P.R. Nelson. 2018b. The effects of tropical cyclone-generated deposition on the sustainability of the Pearl River Marsh, Louisiana: The importance of the geologic framework. *Frontiers in Ecology and Evolution* 6: 179.

National Oceanic and Atmospheric Administration (NOAA), 2018a website: <https://coast.noaa.gov/hurricanes/>. Date of retrieval: June 2018a

National Oceanic and Atmospheric Administration (NOAA), 2018b Hurricane Harvey imagery, website: <https://storms.ngs.noaa.gov/storms/harvey/index.html#15/28.8968/-95.5174>. Date of retrieval: June 2018b

Rachel J., 2018 San Bernard National Wildlife Refuge handbook of Texas online, accessed July 11, 2018: <http://www.tshaonline.org/handbook/online/articles/gks03>.

Ramírez-Herrera, M.T., M. Lagos, I. Hutchinson, V. Kostoglodov, M.L. Machain, M. Caballero, A. Goguitchaichvili, B. Aguilar, C. Chagué-Goff, J. Goff, and A.C. Ruiz-Fernández. 2012. Extreme wave deposits on the Pacific coast of Mexico: tsunamis or storms?—A multi-proxy approach. *Geomorphology* 139: 360–371.

Ryu, J., T.A. Bianchette, K.B. Liu, Q. Yao, and K.D. Maiti. 2018. Palynological and geochemical records of environmental changes in a *Taxodium* swamp near Lake Pontchartrain in Southern Louisiana (USA) during the last 150 years. *Journal of Coastal Research Special Issue* 85: 381–385.

Texas Parks and Wildlife (TPWD), 2018 website: [https://tpwd.texas.gov/publications/pwdpubs/pwd\\_rp\\_t3200\\_1059c/san\\_bernard\\_river.phtml](https://tpwd.texas.gov/publications/pwdpubs/pwd_rp_t3200_1059c/san_bernard_river.phtml). Date of retrieval: June 2018.

The United States Geological Survey (USGS), 2018 website: <https://waterdata.usgs.gov/usa/nwis/uv>. Date of retrieval: June 2018.

The World's Storm Surge Data Center (SURGEDAT), 2018 website: <http://surge.srcc.lsu.edu>. Date of retrieval: June 2018.

U.S. Fish and Wildlife Service (FWS). 2010 Annual report of lands under control of the U.S. Fish and Wildlife Service. Website: <https://www.fws.gov/refuges/land/LandReport.html>. Date of retrieval: July 30, 2019.

van Soelen, E.E., G.R. Brooks, R.A. Larson, J.S.S. Damsté, and G.J. Reichart. 2012. Mid- to late-Holocene coastal environmental changes in southwest Florida, USA. *The Holocene* 22: 1–10.

Wallace, D.J., and J.B. Anderson. 2010. Evidence of similar probability of intense hurricane strikes for the Gulf of Mexico over the late Holocene. *Geology* 38 (6): 511–514.

Wallace, D.J., J.D. Woodruff, J.B. Anderson, and J.P. Donnelly. 2014. Paleohurricane reconstructions from sedimentary archives along the Gulf of Mexico, Caribbean Sea and western North Atlantic Ocean margins. *Geological Society, London, Special Publications* 388 (1): 481–501.

Wang, L., T.A. Bianchette, and K. Liu. 2019. Diatom evidence of a paleohurricane-induced coastal flooding event in Weeks Bay, Alabama, USA. *Journal of Coastal Research* (in press).

Westerhoff, P., P. Chao, and H. Mash. 2004. Reactivity of natural organic matter with aqueous chlorine and bromine. *Water Research* 38 (6): 1502–1513.

Williams, H.F. 2010. Storm surge deposition by Hurricane Ike on the McFaddin National Wildlife Refuge, Texas: Implications for paleotempestology studies. *Journal of Foraminiferal Research* 40: 210–219.

Williams, H.F.L. 2012. Magnitude of Hurricane Ike storm surge sedimentation: Implications for coastal marsh aggradation. *Earth Surface Processes and Landforms* 37: 901–906.

Williams, H.F.L., and W.M. Flanagan. 2009. Contribution of Hurricane Rita storm surge deposition to long-term sedimentation in Louisiana coastal woodlands and marshes. *Journal of Coastal Research Special Issue* 56: 1671–1675.

Yao, Q., and K.B. Liu. 2017. Dynamics of marsh-mangrove ecotone since the mid-Holocene: A palynological study of mangrove encroachment and sea level rise in the Shark River Estuary, Florida. *PLoS One* 12 (3): e0173670.

Yao, Q., and K.B. Liu. 2018. Changes in modern pollen assemblages and soil geochemistry along coastal environmental gradients in the Everglades of south Florida. *Frontiers in Ecology and Evolution* 5: 178.

Yao, Q., K.B. Liu, V.H. Rivera-Monroy, and W.J. Platt. 2015. Palynological reconstruction of environmental changes in coastal wetlands of the Florida Everglades since the mid-Holocene. *Quaternary Research* 83: 449–458.

Yao, Q., K.B. Liu, and J. Ryu. 2018. Multi-proxy characterization of Hurricane Rita and Ike storm deposits in a coastal marsh in the Rockefeller Wildlife Refuge, Southwestern Louisiana. *Journal of Coastal Research Special Issue* 85: 841–845.

You, A.Z. 2008. Comparative study of chemical composition of sediments from different water systems and estuaries of Fujian province. *Geophysical and Geochemical Exploration* 32: 28–30.